Giant enhancement of luminescence intensity in Er-doped Si/SiO_2 resonant cavities

E. F. Schubert, A. M. Vredenberg, N. E. J. Hunt, Y. H. Wong, P. C. Becker, J. M. Poate, D. C. Jacobson, L. C. Feldman, and G. J. Zydzik
AT&T Bell Laboratories, Murray Hill, New Jersey 07974

(Received 8 May 1992; accepted for publication 14 July 1992)

Si/SiO_2 Fabry–Pérot microcavities with rare-earth-doped SiO_2 active regions are realized for the first time. Cavity-quality factors exceeding $Q=300$ are achieved with structures consisting of two Si/SiO_2 distributed Bragg reflectors and an Er-implanted $(\lambda/2)$ SiO_2 active region. The room-temperature photoluminescence intensity of the on-axis emission is 1–2 orders of magnitude higher for resonant cavity structures as compared to structures without a cavity.

The spontaneous emission of photons due to electronic transitions in condensed matter systems depends on the characteristics of the initial and final electronic state and on the optical mode density. The spontaneous radiative transition rate is given by[1]

$$W_{\text{spont}}=\tau_{\text{spont}}^{-1}=\int_0^\infty W_{\text{spont}}^{(l)}\,p(\nu_l)\,d\nu_l, \qquad (1)$$

where $W_{\text{spont}}^{(l)}$ is the spontaneous transition rate into an optical mode l and $p(\nu_l)$ is the optical mode density. In free space, the optical mode density is given by[1]

$$p(\nu_l)=8\pi\nu_l^2 n^3 V/c^3, \qquad (2)$$

where n, V, and c are the refractive index, the volume of the medium, and the velocity of light, respectively. In free space, the optical mode density is a continuous function of the mode frequency ν_l. This situation is changed in one-dimensional (1D) Fabry–Pérot cavities. In such cavities, the mode density is "quantized," i.e., only specific modes can exist inside the cavity. For a 1D cavity consisting of two coplanar reflectors, the wavelengths of the modes, λ_l, of the cavity are given by

$$2L_z=N\lambda_l+\frac{\lambda_l}{2\pi}\phi_1(\lambda_l)+\frac{\lambda_l}{2\pi}\phi_2(\lambda_l), \qquad (3)$$

where N is an integer, and $\phi_1(\phi_l)$ and $\phi_2(\lambda_l)$ are the phase shifts of the reflected waves incurred at the two reflectors of the cavity. The spectral broadening of the modes depends on the reflectivities of the two reflectors and on the cavity length L_z and can be expressed, for example, by the uncertainty relation. The changes in spontaneous emission characteristics in 1D cavities have been known and demonstrated some time ago.[2] In addition to 1D cavities, 3D periodic dielectric structures were proposed to change spontaneous emission in solid-state structures.[3] More recently, changes of the spontaneous emission characteristics were demonstrated in 1D semiconductor systems and include changes in spectral purity, lifetime, and emission intensity.[4–6]

In this letter, we report for the first time on the spontaneous emission characteristics from Er in a Si/SiO_2 cavity. The cavity consist of two Si/SiO_2 distributed Bragg reflectors and a SiO_2 active region. Er is incorporated into the center SiO_2 layer by ion implantation. Recently, Polman *et al.*[7] demonstrated that MeV Er implantation can be used to incorporate Er at high concentrations (e.g., 0.1 at. %) with long lifetimes (e.g., 10 ms) in SiO_2. The cavity wavelength is in resonance with the 1.55 μm emission of a $4f$ electronic transition of Er^{3+} ions in SiO_2.[8] As a consequence, the emission characteristic of the Er is drastically changed, including the emission intensity and the spectral purity, as compared to a no-cavity structure.

A schematic illustration of the Er-implantation profile and the layer sequence of the cavity is shown in Fig. 1. The cavities consist of a bottom distributed Bragg reflector, a SiO_2 active region, and a top distributed Bragg reflector. The bottom and top reflectors consist of 4 and $2\frac{1}{2}$ pairs of Si ($\lambda/4\cong 1150$ Å) and SiO_2 ($\lambda/4\cong 2700$ Å) quarter-wave layers, respectively. The calculated reflectivities of the bottom and top reflectors are 99.8% and 98.5%, respectively. The active region has a thickness of 5400 Å. The Si layers are deposited by dc-magnetron sputtering at a rate of 125 Å/s. The SiO_2 layers are deposited by rf-magnetron sputtering at a rate of 30 Å/s. After growth of the full structure, the reflectivity is measured using a tungsten halogen light source and an optical spectrum analyzer. Subsequently, a 1 cm^2 area is implanted with Er at a dose of 7.7×10^{15} cm^{-2} and an implantation energy of 3.55 MeV. The projected range of the implant is 1.15 μm, i.e., the maximum of the Er concentration occurs in the center of the SiO_2 active region. The projected straggle of the implant is 2450 Å. Post-implantation anneals are carried out at 700–900 °C for 30 min. Photoluminescence measurements are carried out at room temperature using a Ti/sapphire laser tuned to an excitation wavelength of 980 nm. Finally, the top mirror on some of the samples is removed by wet chemical etching. The employment of highly selective etches allows for the selective removal of the top mirror only. This procedure makes possible the comparison of structures with and without cavity on the *same* Er-implanted sample.

The resonance between the cavity mode and the emission wavelength of the Er is of critical importance. The emission from Er is due to a transition between atomic $4f$ levels which is inherently narrow. However, the Er-emission lines are inhomogeneously broadened by the random local environment of Er^{3+} ions in the SiO_2 host. The Er emission occurs typically between 1500 and 1600 nm with two distinct maxima at 1535 and 1550 nm. The re-

Downloaded 17 Apr 2002 to 128.197.178.239. Redistribution subject to AIP license or copyright, see http://ojps.aip.org/aplo/aplcr.jsp

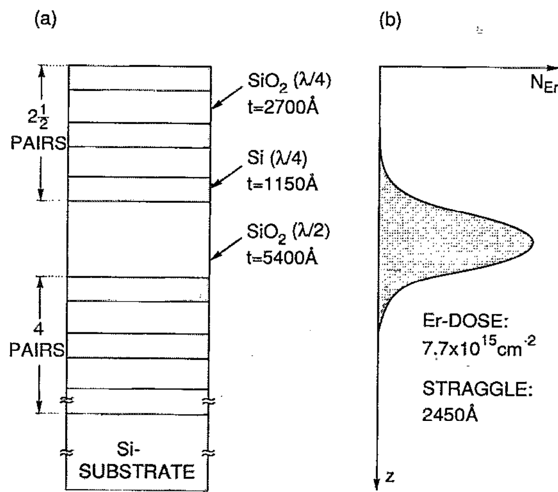

FIG. 1. (a) Schematic structure of the Si/SiO_2 resonant cavity structure and (b) the Er-implantation profile.

flectivity spectrum of a Si/SiO_2 cavity is shown in Fig. 2. The reflectivity spectrum was measured using fibre-guided optics under near-normal incidence conditions. The reflectivity spectrum shown in Fig. 2 exhibits interference fringes at wavelengths <1150 nm and a very high reflectivity band for wavelengths >1200 nm. At a wavelength of 1.54 μm, a dip in the reflectivity is observed, indicating the resonance mode of the cavity. We note that a highly accurate control of the growth process is required in order to obtain the desired resonance wavelength. Since the resonance wavelength depends linearly on the layer dimensions, a layer dimensions control better than 1% is required. The transmission resonance is shown in greater detail in the inset of Fig. 2. The magnitude of the dip is 3 dB and its full width at half maximum (FWHM) is $\Delta\lambda=5$ nm. The cavity quality factor Q can be inferred from the width of the transmission resonance using

$$Q=\lambda/\Delta\lambda, \tag{4}$$

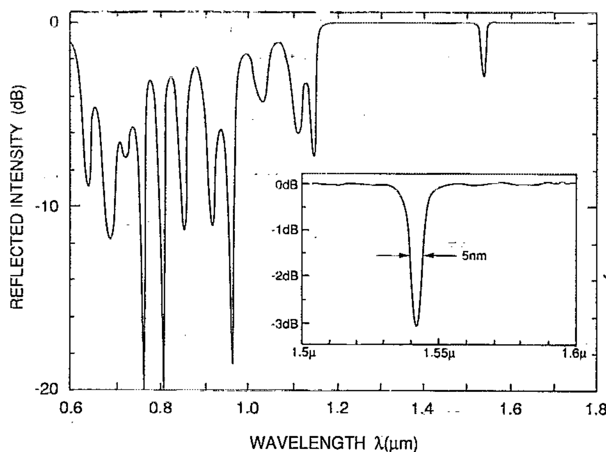

FIG. 2. Reflectivity of a Si/SiO_2 Fabry–Pérot cavity with 4 pairs of Si/SiO_2 bottom mirrors, a $\lambda/2$ SiO_2 active region, and a $2\frac{1}{2}$ pairs Si/SiO_2 top mirrors grown on a Si substrate.

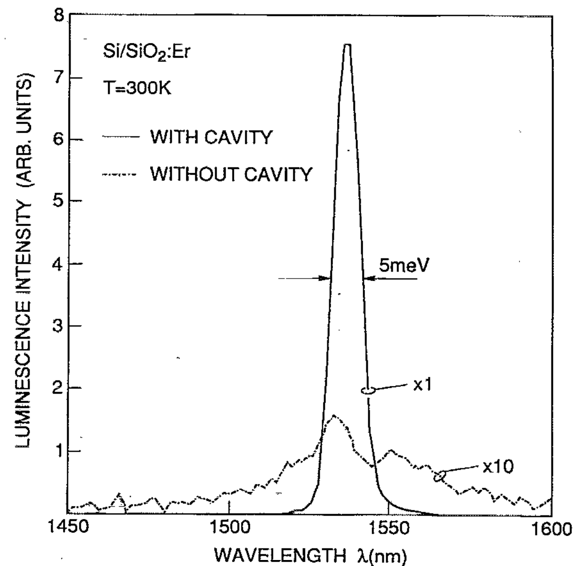

FIG. 3. Room-temperature photoluminescence spectra of Er-implanted Si/SiO_2 structures with and without resonant cavities.

where λ is the wavelength of the resonance. A value of $Q=310$ is inferred from Eq. (4).

The top mirror of some samples was removed by selective wet chemical etching on some parts of the sample. The removal of the top mirror allows us to make direct comparisons between structures with and without a cavity. Note that most of the implanted Er is located in the center SiO_2 layer of the cavity. The Er located in the top-mirror SiO_2 layer is less than 7% of the total Er density as inferred from the active layer thickness of 5400 Å and a projected straggle of 2450 Å. The Er located in the Si of the top mirror luminesces only weakly.[8] Therefore, the removal of the top mirror does not significantly reduce the amount of optically active Er in the structure.

The comparison of photoluminescence spectra measured at normal incidence of Er-doped SiO_2 structures with and without a resonant cavity is shown in Fig. 3. Most strikingly, the peak intensity of the resonant cavity structure is greatly enhanced as compared to the structure without a cavity. For the samples shown in Fig. 3, the increase in intensity is a factor of 50. The enhancement in intensity studied on different samples is typically one to two orders of magnitude. We attribute the enhancement entirely to the presence of the resonant cavity. The enhancement can be calculated from the finesse of the cavity. For δ-functionlike emission spectra occurring at the resonance wavelength of the cavity, the enhancement factor is given by the finesse of the cavity[9]

$$F=\frac{\pi(R_1R_2)^{1/4}}{1-\sqrt{R_1R_2}}. \tag{5}$$

Using $R_1=98.5\%$ and $R_2=99.8\%$, the finesse is calculated to be $F=370$. The experimental finesse (F=310) is smaller than the calculated one, possibly due to thickness variations of the reflector layers which reduce the reflectivity. Furthermore, a direct comparison of the photolumi-

Downloaded 17 Apr 2002 to 128.197.178.239. Redistribution subject to AIP license or copyright, see http://ojps.aip.org/aplo/aplcr.jsp

nescence of the two structures is complicated by the bottom reflector of the structure without a cavity, which enhances the emission through the top by approximately a factor of 2.

The change in emission intensity is *not* due to different excitation conditions of the structures with and without a cavity. First, some of the exciting light ($\lambda = 980$ nm) is absorbed in the Si layers of the top mirror. The top mirror therefore causes a *weaker* excitation of the active region in the cavity as compared to the structure without a top reflector. Second, the excitation wavelength ($\lambda = 980$ nm) is far off resonance. We therefore attribute the change in emission characteristic entirely to the effect of the resonant cavity.

In addition to the change in luminescence intensity, Fig. 3 also reveals a significant change in the spectral purity of the Er emission. The photoluminescence has a clean, symmetric line shape, with a FWHM of 5 meV (10 nm). The Er emission spectrum of the structure without a cavity is broader, typically 20-meV wide, and has a double-peak structure. The change in spectral characteristics indicates that the near normal emission is mainly determined by the characteristics of the cavity rather than the inhomogeneously broadened emission of Er-doped SiO_2.

The spontaneous emission from the resonant cavity is strongly directed along the optical axis of the cavity. Note that such a directed emission is desirable in optical fibre applications for high coupling efficiencies. In order to investigate the angular dependence of the emission, photoluminescence spectra were taken for normal and off-normal directions. The emission wavelength as a function of the emission angle is shown in Fig. 4. For off-normal angles, the emission wavelength shifts to *shorter* wavelengths, i.e., higher energies. The shift can be understood in terms of a constant, on-resonance energy of the on-axis component of the radiation mode. Assuming a constant on-axis energy of photons, the emission wavelength in air ($n_{\text{air}} = 1$) originating from a cavity consisting of an active medium with index n and two planar (nondistributed) mirrors can be expressed as a function of the emission angle θ_0

$$\lambda_e = \lambda_{\text{res}} \cos \left[\arcsin \left(\frac{1}{n} \sin\theta_0 \right) \right], \tag{6}$$

where λ_{res} is the resonance wavelength of the cavity. For small angles, Eq. (6) can be approximated by

$$\lambda_e \cong \lambda_{\text{res}} \left(1 - \frac{1}{2} \frac{\theta_0^2}{n^2} \right). \tag{7}$$

Equations (6) and (7) are shown in Fig. 4 for $\lambda_{\text{res}} = 1.555$ μm and $n = 1.5$ by the solid and dashed line, respectively. Note that Eqs. (6) and (7) apply to cavities with thin, coplanar mirrors. For distributed Bragg reflectors, an *ef-*

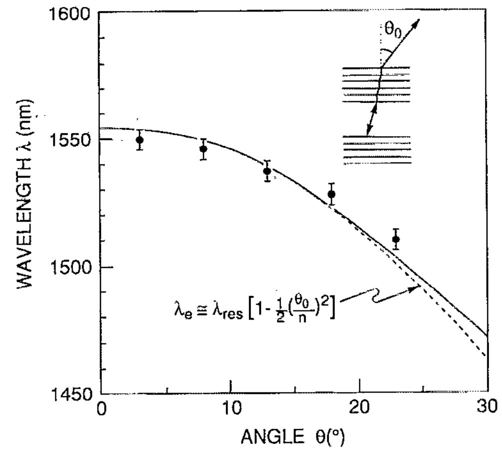

FIG. 4. Emission wavelength of an Er-doped Si/SiO_2 resonant cavity as a function of the emission angle. The solid and dashed lines are calculated emission wavelengths assuming a constant energy of the on-axis component of the optical wave.

fective index, n_{eff}, must be substituted for n. For the structure discussed here, we have $n_{\text{eff}} > n$, which reduces the dependence of λ_e on θ_0 [as compared to Eqs. (6) and (7)]. In addition to the change in wavelength, a drop in intensity is observed with increasing angle. For example, the intensity drops by a factor of 15 by changing the emission angle from 13° ($\lambda_e = 1.537$ μm) to 23° ($\lambda_e = 1.510$ μm).

In conclusion, we have realized Er-implanted Si/SiO_2 resonant Fabry–Pérot cavities consisting of ($\lambda/2$) SiO_2 active regions and two Si/SiO_2 distributed Bragg reflectors. Cavity-Q values of 310 and finesses of 73 are inferred from the optical characteristics of the structure. Photoluminescence at room temperature reveals a drastic enhancement of the luminescence intensity emitted along the optical axis of the cavity. The intensity of the cavity structures is typically 1–2 orders of magnitudes higher as compared to structures without a cavity. Furthermore, the emission wavelength and the intensity decrease for off-normal emission angles. The change in emission wavelength can be quantitatively described by assuming the on-axis component of the optical wave is resonant with the cavity.

[1] A. Yariv, *Theory and Applications of Quantum Mechanics* (Wiley, New York, 1982), p. 143.
[2] E. M. Purcell, Phys. Rev. **69**, 681 (1946).
[3] E. Yablonovitch, Phys. Rev. Lett. **58**, 2059 (1987).
[4] H. Yokoyama, K. Nishi, T. Anan, H. Yamada, S. D. Brorson, and E. P. Ippen, Appl. Phys. Lett. **57**, 2814 (1990).
[5] M. Suzuki, H. Yokoyama, S. D. Brorson, and E. P. Ippen, Appl. Phys. Lett. **58**, 998 (1991).
[6] E. F. Schubert, Y.-H. Wang, A. Y. Cho, L.-W. Tu, and C. J. Zydzik, Appl. Phys. Lett. **60**, 921 (1992).
[7] A. Polman, D. C. Johnson, D. J. Eaglesham, R. C. Kistler, and J. M. Poate, J. Appl. Phys. **70**, 3778 (1991).
[8] W. J. Miniscalco, J. Lightwave Technol. **9**, 234 (1991).
[9] X.-P. Feng and K. Ujihara, Phys. Rev. A **41**, 2668 (1990).

Downloaded 17 Apr 2002 to 128.197.178.239. Redistribution subject to AIP license or copyright, see http://ojps.aip.org/aplo/aplcr.jsp